Slowing of Oxidation for Aluminum Thin-Films through use of High-Volume Oxygen Absorbers

Kendall Mitchell

A thesis submitted to the faculty of
Brigham Young University
in partial fulfillment of the requirements for the degree of

Bachelor of Science

David Allred, Advisor

Department of Physics and Astronomy

Brigham Young University

April 2023

ABSTRACT

Slowing of Oxidation for Aluminum Thin-Films through use of
High-Volume Oxygen Absorbers

Kendall Mitchell

Department of Physics and Astronomy, BYU

Bachelor of Science

Aluminum is a great potential material for thin-film mirrors in space telescopes as it has a high reflectance range. However, when aluminum oxidizes, the reflectance range no longer includes light beyond ~120 nm wavelengths as the reflectivity drops below 5%. In order to maximize reflectance in the ultraviolet and open potential data such as Lyman series lines, there needs to be a way to keep that high reflectance range. This research explores potential storage environments that slow the oxidation of thin aluminum films through use of oxygen absorbers, where the film and oxide thicknesses are tracked through use of ellipsometry. Results show that 3000 cubic centimeters (cc) of oxygen absorbers can slow the oxidation of aluminum samples by 3.6 times, 6000 ccs by 3.0 times, 9000 ccs by 2.4 times.

Keywords: Aluminum thin-films, oxygen absorbers, ellipsometry

ACKNOWLEDGMENTS

I would like to acknowledge Dr. David Allred for the immense guidance and direction he provided during my time at BYU both in studies and research. I thank Donovan Smith for the creation of the python script to assist in analyzation. Also Dr. Matthew Linford for use of the ellipsometer which was the primary instrument used for data collection and analysis.

Contents

List of Figures

Chapter 1

Introduction

1.1 Aluminum Thin-Films

During the 2020 Astrophysics Decadal Survey, the three primary motivations forwarding the next decade of experimentation were better understanding planet star relations, discovering new particles, and studying the origins of the universe. In order to accomplish these goals, several proposals from NASA including the Large UV/Optical/IR Surveyor (LUVOIR) and the Habitable Exoplanet Observatory (HabEx), need to be able to observe electromagnetic waves through the XUV to IR. (National Academies of Sciences, Engineering, and Medicine, 2021) Specifically, the mirrors for these proposed projects need mirrors that can observe the Lyman ultraviolet range (LUV) between 91.2 nm through 121.6 nm for the hydrogen spectral lines.

Aluminum (Al) is the best candidate thin-film material for broadband mirrors because of the unmatched high reflectance in the extreme ultraviolet (XUV) wavelengths through infrared (IR), keeping 80% past 90 nm wavelengths. (Larruquert, 1995) Currently, the Hubble Space Telescope (HST) possesses the furthest UV reflectance we have, but only with 15% reflectance at wavelengths shorter than 110 nm. This is due to the necessary 25 nm magnesium fluoride

(MgF_2) layer coating the aluminum. (Fleming, 2017) Because telescopes use mirrors in series, the final reflection of intensity for wavelengths in the mentioned range can be several magnitudes lower than 15%. Metal fluoride layers are necessary because they prevent the oxidation of aluminum better than other examined layers. (Méndez, 2000) (Hunter, 1971) A thin layer of aluminum oxide (Al_2O_3), even only 1 nm thick, can cause the reflectance to drop from 90% to 20% below 150 nm. (Madden, 1963) (Fleming, 2017) Besides the fact that aluminum oxidizes almost immediately, (Turley, 2017) before the projects would be launched into space, they will be stored for long periods of time, likely years. Because of this, the need for a fluoride coat is certain.

1.2 Potential of Oxygen Absorbers

Our group has experience studying the oxidation of aluminum under various coatings, including aluminum fluoride (AlF_3) and lithium fluoride (LiF) as well as MgF_2. (Davis, 2017) (Miles, 2017) (Allred, 2017) We observed that oxidation still occurs underneath metal fluoride coatings, and although the oxidation is much slower, the aluminum still oxidizes fully if the sample remains in ambient conditions for long periods of time. Thus, there is a need for an efficient storage method for mirror samples. Both for the purpose of proposed projects as well as standardizing measurements between collaborating labs. Currently when we ship or receive samples, the samples have changed optically due to oxidization. An efficient storage solution could standardize measurements between labs and allow for thinner metal fluoride layers, thus preventing a further drop of reflectance in the XUV. Research suggests that a 2-3 nm layer of

AlF_3 rather than 25 nm of MgF_3 could raise reflectance in XUV, therefore allowing us to see further than HST. (Hennessy, 2016)

In order to evaluate storage environments more effectively this experiment utilizes bare aluminum samples rather than aluminum with a metal fluoride layer. This is both to save time and to allow for more accurate characterization of measurements. The candidate for storage examined is high volumes of iron powder oxygen absorbers coupled with aluminized vacuum seal bags. Previous experiments show the potential of liquid nitrogen, dry ice, and argon storage environments. Although each had impressive results, the cryogens require maintenance and would be difficult for shipping purposes, while the argon had difficulty consistently acquiring an effective seal. Oxygen absorbers are inexpensive, and if coupled with vacuum sealed bags, could provide ample means to prevent oxidation for a long period of time without maintenance or creating a potentially hazardous environment. Experimentation shows that in food storage, oxygen absorbers coupled with oxygen impermeable packaging can lower the oxygen concentration to below 100 ppm. (Cichello, 2015) If aluminum mirror samples with oxygen absorbers can reach those levels of oxygen reduction, then that makes oxygen absorbers much more appealing for storing and shipping.

Chapter 2

Methods

2.1 Thermal Evaporation

The aluminum thin film samples are created using thermal evaporation in a glass bell-jar (1) thermal evaporator (Fig. 1). The glass bell jar used to create the vacuum seal is brought to atmospheric pressure using nitrogen gas, then raised. The sample platen (2) is extracted where we place the sample substrate (3) of silicon dioxide (SiO_2) on silicon. The substrate is attached to the plate using screws and washers, then the plate gets placed back into the chamber. The shutter (4) is ensured to be covering the sample substrate. The Inficon quartz-crystal thickness monitor (QCM) (5) is checked to make sure it still is not completely covered and can still read out thicknesses. The aluminum is then placed in a tungsten filament boat (6) which is attached to two metal leads. The bell jar is then closed and sealed and the chamber is brought down to 5 mircoTorr by cryogenic vacuum (7). Then the leads attached to the boat have a current driven through them and the aluminum is heated inside the boat and begins to evaporate. Using the QCM, we monitor the evaporation rate until it reaches the desired speed then the shutter is turned and the aluminum deposited until the appropriate thickness is reached. The thickness also being

measured via QCM. The shutter then covers the substrate, the current turned off, and the boat allowed to cool before pressure is restored to the chamber and the bell jar raised. After the newly deposited aluminum samples were created, they were quickly cut, measured, and placed into storage to prevent total oxidation.

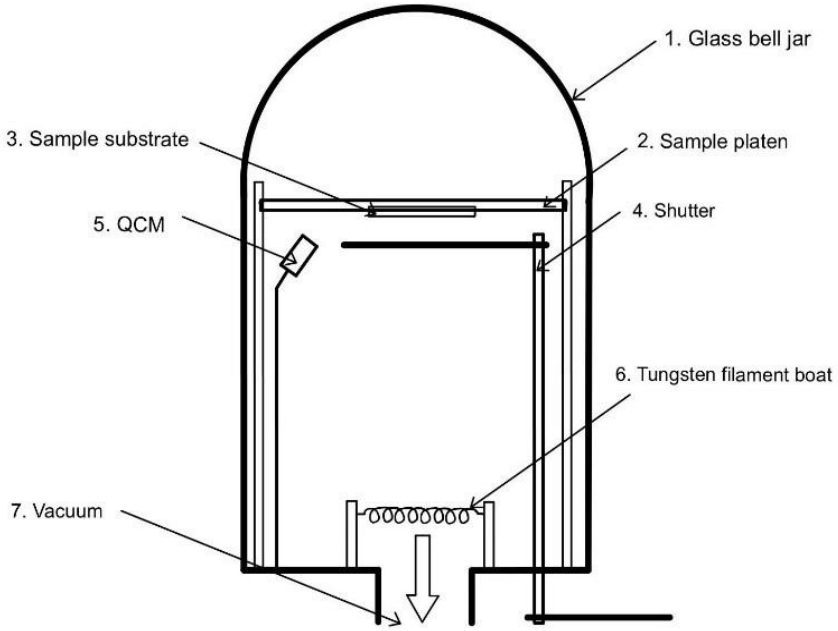

Figure 1: Thermal evaporation chamber used to deposit 20-30 nm of aluminum onto a SiO_2 substrate. The evaporation rate needs to be fast (2-3 nm per second) in order to prevent oxide formation inside the aluminum.

During evaporation for aluminum, it is best if the evaporation rate is as fast as possible to prevent oxide from forming inside the aluminum layer. (Egan, 2017) The accomplished evaporation rate was between 2-3 nm/s. The aluminum used was 99.9% pure Al wire. The samples cut from the wafers were approximately 30 mm by 30 mm squares. The substrate thickness for the CVD SiO_2 was between 350-430 nm.

2.2 Ellipsometric Characterization

In order to track the thickness of Al_2O_3, constant measurements were required. Immediately after evaporation the samples were measured for initial thickness through use of the JA Woollam Model RC2 variable-angle, spectroscopic ellipsometer (VASE). Ellipsometric measurements and characterization were done using VASE from a 193-1690 nm wavelength range. This wavelength range was measured for Psi amplitude, which is a constant proportional to the ratio of the Fresnel coefficients of p and s polarized light axis, at angles of incidence every 5 degrees between 60° to 80°. Characterization was done using the CompleteEASE software from J.A. Woollam to measure the sample specific thicknesses for Al_2O_3, aluminum, and SiO_2. Characterization consisted of creating a model of layers using Woollam's database of various materials (Fig. 2). A fit was then created in the program which changes the thicknesses of the model to fit the data best. The fit Mean Square Error (MSE) is how one gauges if the thicknesses are accurate, with an MSE below 8 being an acceptable fit for samples on SiO_2.

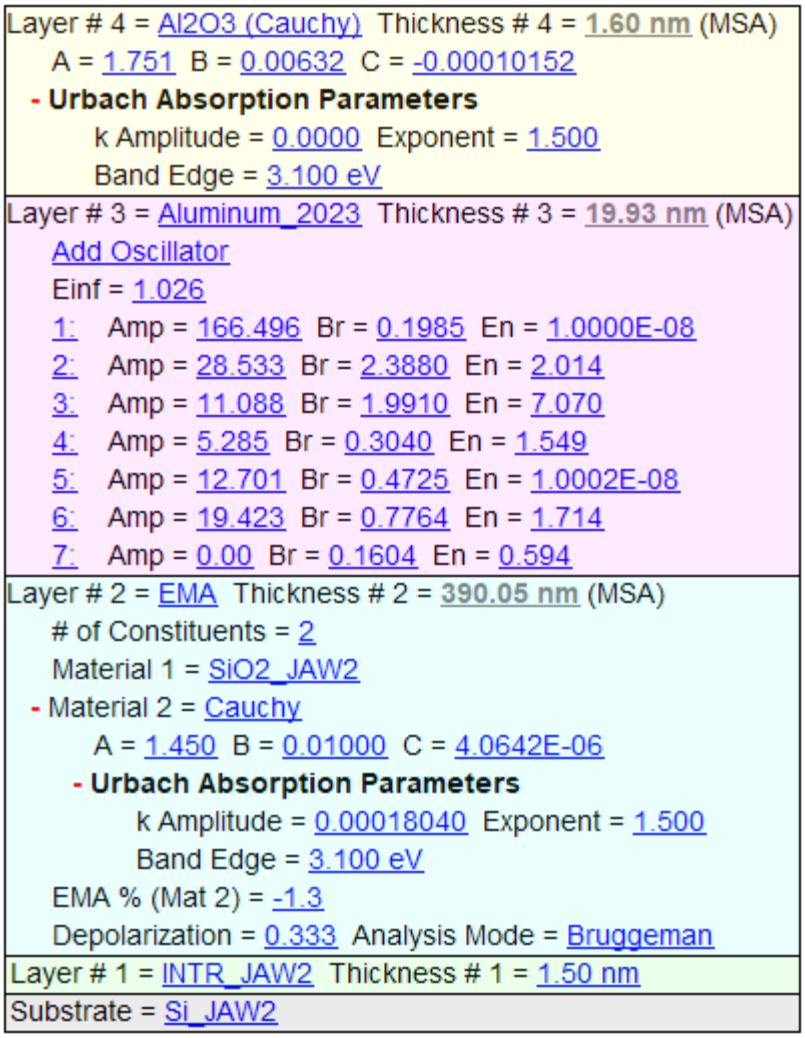

Figure 2: Detailed view of model used to measure oxide thickness. Multi-sample analysis (MSA) was used for the three primary layers and one can see here the specific optical parameters used.

The bottom layer is the silicon substrate with SiO_2 deposited on top along with an intermix layer between the two. The purpose of the intermix layer is to account for imperfections from deposition and reactions between the Si and SiO_2 layer. The SiO_2 layer originally was a simple tabulated layer with fixed parameters. This proved not fit as we would like, with the model being offset in the UV range, so it was replaced with an effective medium approximation (EMA) layer split between the fixed parameter SiO_2 material and a simple Cauchy layer. This way the parameters and percentage of SiO_2 to Cauchy layer could be changed and the model fit much better, especially in the UV. The desired aluminum thickness was around 400 nm to allow for several fringe packets between the UV to IR range.

The next layer is aluminum. The aluminum was modeled using 7 gaussian oscillators where we allowed the individual oscillators to fit one at a time for each sample. This was done because the deposition of the aluminum changes the optical properties across the whole sample, so every sample of aluminum was slightly different. The gaussian oscillators were placed throughout the measured range to simulate peaks in reflectance for aluminum. The gaussians would fit around 0 eV (1690 nm), 1.5 eV (825 nm), and 7 eV (175 nm). The 7^{th} gaussian oscillator often was not necessary and would fit to have 0 amplitude. The desired thickness of the aluminum was between 18-30 nm because any less than this and the aluminum begins to become too transparent, making fitting the model and measuring oxide difficult. Any more than 30 nm and the aluminum begins to become to opaque, once again making measuring oxide confidently more difficult.

The final layer is the Al_2O_3 which is a simple parameterized Cauchy material. These parameters were allowed to fit but most commonly would not change. One method tried but not included was the replacement of the Cauchy layer with an EMA layer which included

voids in the oxide growth. This was found to not make a significant impact on the fit and thus was omitted. A roughness of the surface was included and fixed at 1 nm as to not allow the model to replace oxide thickness with roughness instead.

A method used to check the aluminum created is believable was the use of graphing the optical layer properties, those being absorption and index of refraction. For aluminum a very notable peak is present around 1.5 eV (825 nm) which could be used to understand if the parameters changed too much and made the material no longer realistic. Another method was through tracking aluminum and aluminum oxide thicknesses, one could note that for every 1 nm of oxide formed, approximately 0.6 nm of aluminum thickness should have gone down because that aluminum reacted and became aluminum oxide. When the thicknesses of aluminum rise instead of fall as aluminum oxide thickness increases, this was usually a clear indication that something in the model was amiss. The third and most important method was use of the built in mean square error (MSE). The MSE is a goodness of fit number. For samples with SiO_2 substrates the MSE is usually higher because the quick spikes in peaks mean that any slight offset poses a greater effect. So, for these samples, an MSE of below 6 was satisfactory, when normally, an MSE of below 3 is preferred.

The samples were fit using multi-sample analysis (MSA) as each sample oxidized over time. This way the material parameters for the model only needed to be fit once for each sample, then the thickness of the aluminum and aluminum oxide were allowed to change for each measurement. The SiO_2 was also allowed to change for each measurement to account for any slight variations in where the sample was measured, as the ellipsometer only collects optical data for a small area on the sample. Allowing roughness and angle offset to fit for each sample in time

was also considered but found to give unreasonable results, either in unrealistically high angle offset values or the oxide thickness would be replaced with higher roughness values.

2.3 Storage of Samples with Oxygen Absorbers

After initial measurements the samples were cut into 15, 30 by 30 mm squares and split between 3 groups. The samples were placed into 1600 cubic centimeter (cc) aluminized vacuum seal bags with various capacities of oxygen absorbers. The various capacities being 3000 cc, 6000 cc, and 9000 cc. To clarify, the bags were the same size with a volume of 1600 cc, while the maximum oxygen capacity iron powder oxygen absorbers was 3000 cc, 6000 cc, and 9000 cc. It is noted that because atmospheric air is only about 20% oxygen, then the amount of oxygen absorber capacity only needs to be about 400 cc for a 1600 cc container. Higher volumes than necessary are used in this experiment to ensure maximum oxidation reduction. The vacuum seal bags with samples and oxygen absorbers inside were afterwards placed in an ambient lab environment and left for two weeks. After a two-week period, all the samples were removed from storage and resubject to atmospheric conditions.

The samples were measured after thermal evaporation for initial thicknesses of aluminum and aluminum oxide already formed on the surface, which even after only a few minutes can be around 1 nm. Afterwards, they were promptly put into storage and removed after 408 hours. Then the samples were kept in ambient lab conditions so they could oxidize fully. Measurements were taken directly after removal and periodically afterwards to track the oxide thickness. It is well known that rate of oxidation of aluminum decreases as the thickness of the oxide increase,

which makes the thickness versus time trend logarithmic. (Allred, 2017) (Grimblot, 1982) This method of measuring created a full set of data values could be used for a logarithmic fit as the oxidation rate and initial versus fully oxidized values could be compared with the two values of thicknesses before storage and right after storage. The samples then were able to act as their own comparison for oxide growth as many things such as thickness of aluminum and roughness and uniformity affect the growth of oxide.

Chapter 3

Results

3.1 Ellipsometric Analysis

During fitting for the ellipsometric data, it was discovered that the samples had two distinct types of measurements. One set had deep fringes which was expected since the aluminum was on SiO_2 which characteristically has deep fringes. The other set has shallow fringes that have a noticeable upward trend on the Psi amplitude (Fig. 3). This was found to be caused by a thickness nonuniformity in the SiO_2 layer, upwards of 15% across the ~5 mm by 5 mm surface area the ellipsometer measures across. The samples with a higher thickness nonuniformity in the SiO_2 layer had the shallower fringes. An issue presented was that for these samples, any small variation for the location of measurement caused the thicknesses of aluminum and aluminum oxide to shift in unexpected ways, such as the aluminum becoming thicker over time. This is not believable because the aluminum should be shrinking as it reacts and becomes oxidized, meaning that the difference in SiO_2 thickness creates an unrealistic change in the aluminum and subsequently, the aluminum oxide thicknesses. What that means is the aluminum is supposed to shrink at a rate approximately 2/3 of the rate the aluminum oxide

grows. The aluminum and aluminum oxide values then can be determined to be unrealistic if aluminum thicknesses fluctuate greatly while the aluminum oxide growth trend remains slow and consistent.

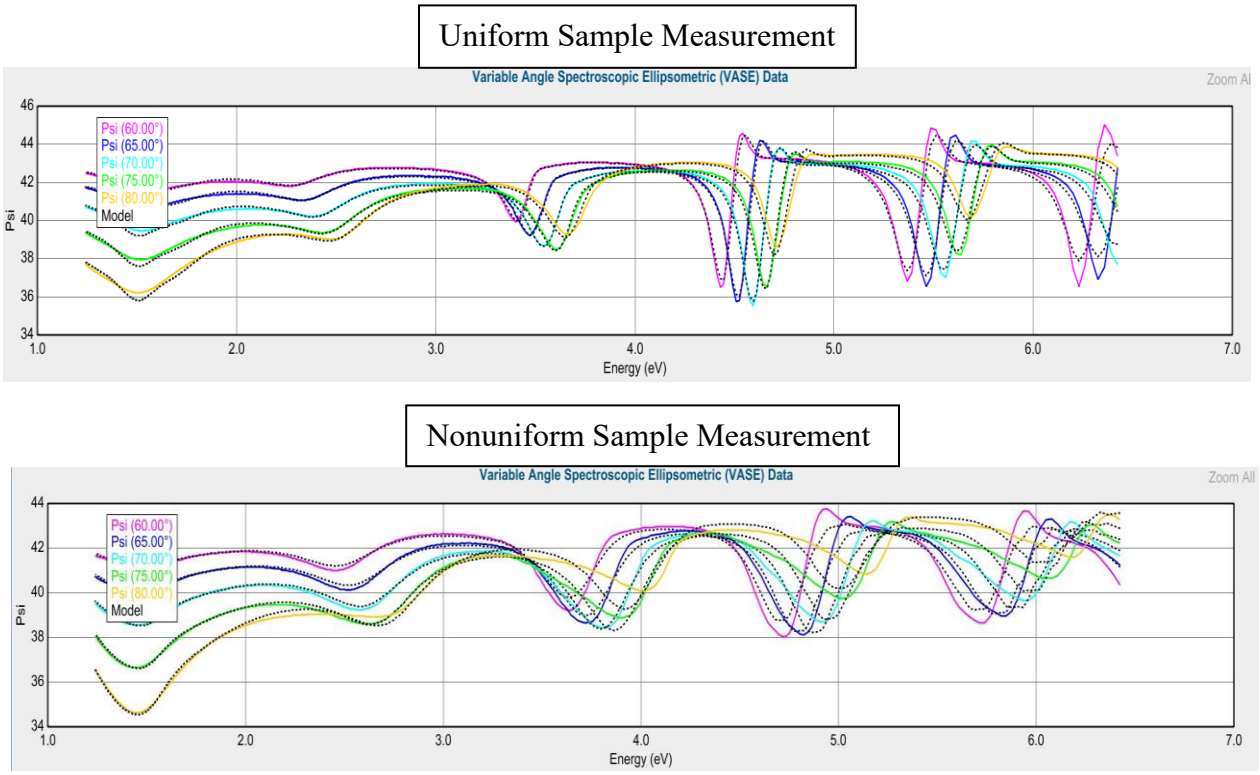

Figure 3: Data collected through VASE relating Psi as a function of photon energy (rather than wavelength). The data shows the difference between uniform and nonuniform data measurements of aluminum deposited on SiO_2. The uniform sample is sharper and has deeper peaks for the Psi scale while the nonuniform sample has rounded shallow peaks. The thicknesses for the uniform data could be collected by using the same SiO_2 thickness and setting the thickness nonuniformity percentage to zero. The data collected in this manner was believable due to the decrease in aluminum thickness being about 60% of the increase in Al_2O_3 thickness. This coupled with a low MSE and the slope of oxidation remaining consistent when other models were applied makes us confident in the data given. The nonuniform thickness is more difficult to fit because it requires allowing SiO_2 and thickness nonuniformity to change for each measurement. This results in a low MSE and a consistent slope as well with those differences added.

From the discrepancy it was concluded that the thickness nonuniformity was likely high for samples taken from the edge of the original SiO_2 wafer. This likely being due to the SiO_2 being deposited on the Si wafer nonuniformly, leading the edges to have large differences in thickness from the center. We were able to shift the model to fit the thickness nonuniformity and SiO_2 layer for every measurement in time. That way those two parameters would be changed in percentage and thickness respectively rather than the aluminum and aluminum oxide being inaccurately altered to account for the shift in thickness nonuniformity.

To improve confidence that this method of shifting the ellipsometric model was correct, two other models were applied to each sample. The first model is described above and includes using MSA for thickness nonuniformity. The second model uses only the tabulated version of SiO_2 JAW included in the CompleteEASE library where the parameters have fixed values and the SiO_2 layer is not included in MSA. The third model uses MSA for SiO_2 JAW as well as MSA for thickness nonuniformity percentage and roughness. The thicknesses given by each of the three models had near equivalent trends and because the first model provided both a lower MSE and a more realistic aluminum to aluminum oxide thickness, it was used to find the thickness of Al_2O_3.

Using multi sample analysis with the aluminum layer, aluminum oxide layer, and if the sample was noticeably nonuniform, including thickness nonuniformity percentage and the SiO_2 layer thickness, data could be characterized confidently. The roughness was fixed at 1 nm in both cases to prevent the Al_2O_3 layer thickness from becoming unrealistically large, which can be noticed when the aluminum oxide is 2-3 nm after only a few minutes. Furthermore, allowing the roughness to fit caused no significant decrease increase in MSE. In this manner every sample was analyzed to track the Al_2O_3 thickness while the aluminum oxidized in air.

3.2 Oxide Growth Trend

It is well known that rate of oxidation of aluminum decreases as the thickness of the oxide increases. Because of this trend, several models were applied to better understand this phenomenon for oxide growth and it was discovered that aluminum oxide growth follows a logarithmic trend. (Allred, 2017) (Grimblot, 1982) In other words, the oxide thickness of the aluminum oxide can be tracked using a logarithmic fit for a time versus thickness. This is important because since the aluminum is in a storage environment, this logarithmic trend will be understandably changed, and no longer resemble a standard logarithmic curve. In order to account for this the time in storage must be offset by an equivalent time in air. This can be found by applying a logarithmic fit, and shifting the points after storage backwards until the R^2 (goodness of fit) value is as close to 1 as possible. For example, if the 408 hours in storage fit best to a logarithmic trend when the data points after storage were subtracted by 380 hours, then equivalent time in air is 28 hours. We name a retardation value (RV) which is the total storage time over the equivalent time in air. For this example, the RV would be 14.6.

The 3000 cc samples were placed in aluminized vacuum seal bags with 3000 ccs of absorption volume in 10 separate 300 cc iron powder oxygen absorbers. The thickness vs. time graph without a retardation factor applied can be found below (Fig. 4). These samples were taken out of storage after 408 hours and then placed in air. Afterwards it oxidized at a rate slower than the time in storage, as expected from data following a logarithmic trend. A logarithmic fit can then be applied and the data shifted by the retardation factor until the R^2 value of the fit was

closest to 1. For this instance, it is found that when the 408 hours in storage is converted to 112 hours, the R^2 value is closest to one and the data set more closely follows a logarithmic trend (Fig. 5). This then provides a value of 3.6±0.4 for the retardation value.

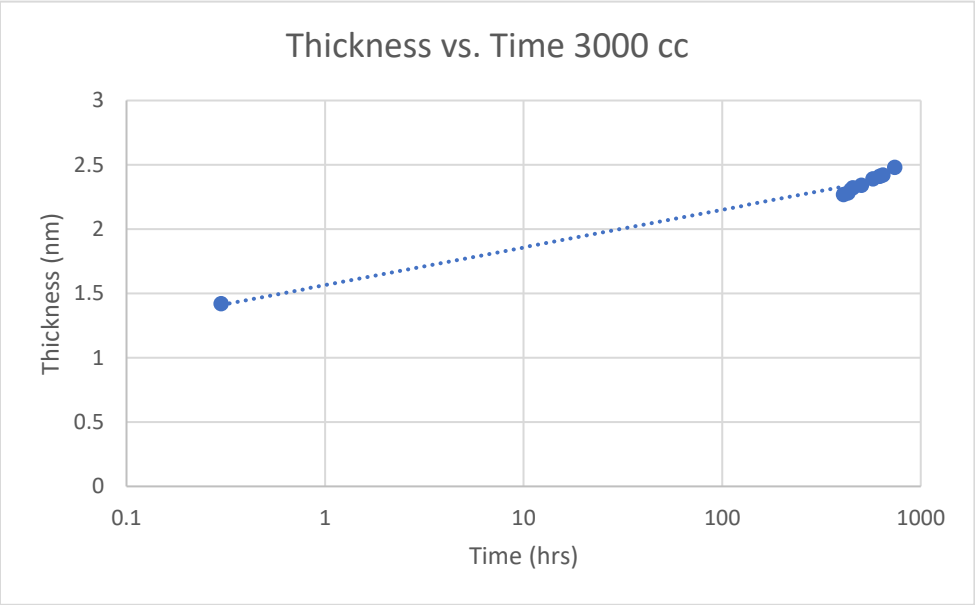

Figure 4: The thickness versus time plot for samples placed in 3000 ccs of oxygen absorbers. Shows the initial fit of the logarithmic curve which although close, is not as good as it can be.

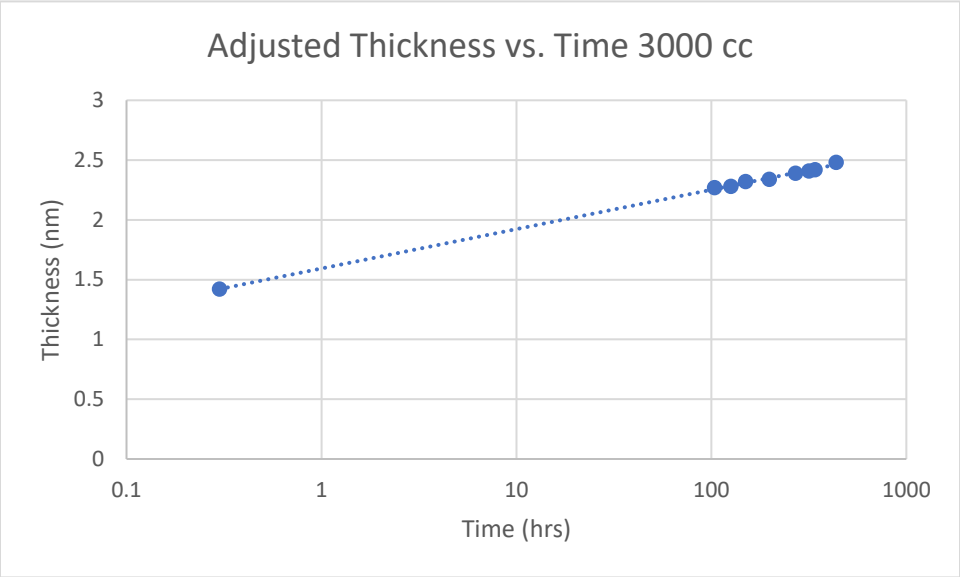

Figure 5: The thickness versus time plot for samples placed in 3000 ccs of oxygen absorbers shifted by a retardation value of 3.6±0.4.

The 6000cc samples were analyzed with the same methodology as the 3000cc samples. Once again, the samples were taken out of storage after 408 hours and allowed to oxidize (Fig. 6). Interestingly, the value of equivalent time in air that this comes out to is 136 hours (Fig. 7). This was the value that gave the best R^2 value for our logarithmic fit. This correlates to a retardation value of 3.0±0.4 for 6000cc's of oxygen absorbers.

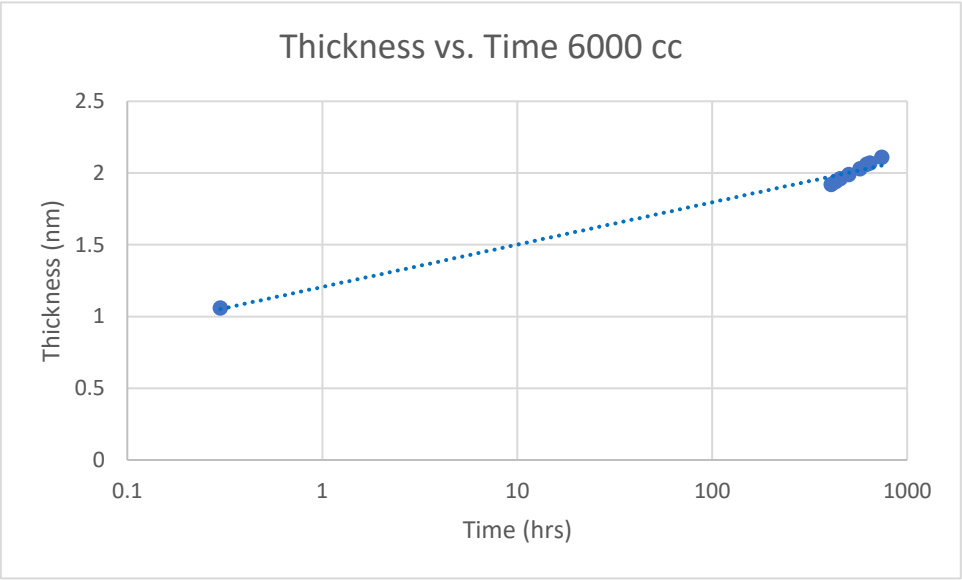

Figure 6: The thickness versus time plot for samples placed in 6000 ccs of oxygen absorbers. Shows the initial fit of the logarithmic curve which although close, is not as good as it can be.

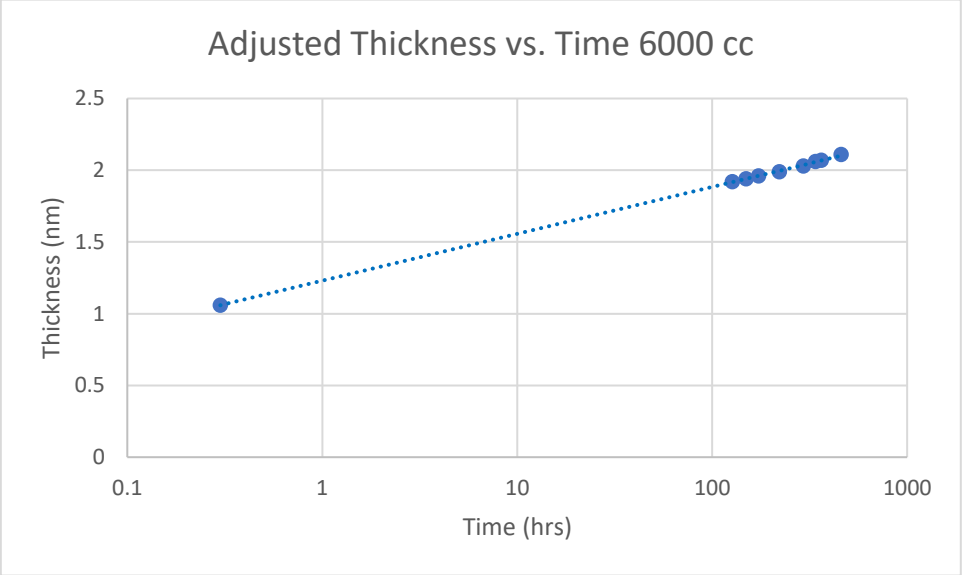

Figure 7: The thickness versus time plot for samples placed in 6000 ccs of oxygen absorbers shifted by a retardation value of 3.0±0.4.

The samples subject to 9000cc's of oxygen absorbers followed the same procedure as 3000cc's and 6000cc's. After being taken out of storage at 408 hours, the samples oxidized and the thickness was measured (Fig. 8). The equivalent time in air was found to be 204 hours, as can be seen (Fig. 9). The retardation factor then is measured to be 2.4±0.3.

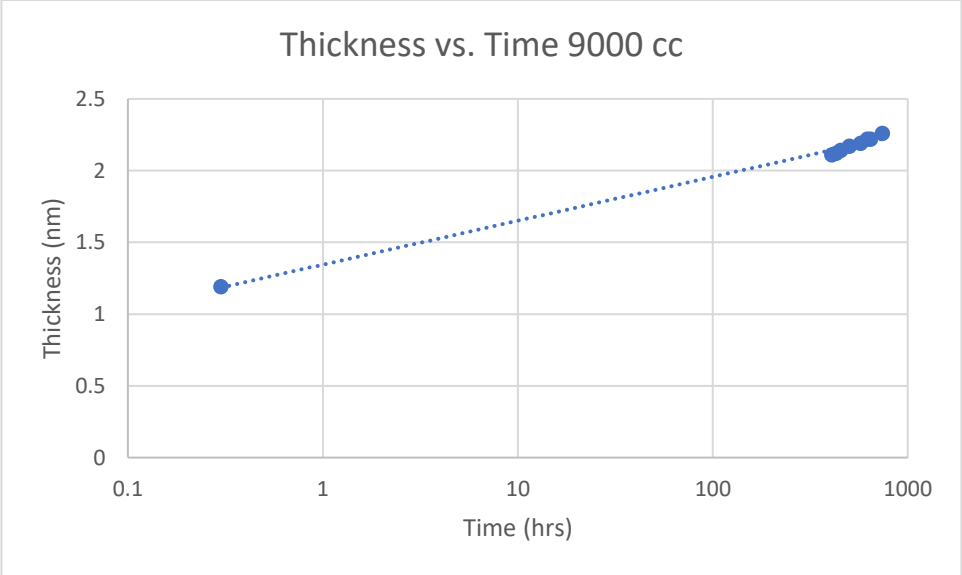

Figure 8: The thickness versus time plot for samples placed in 9000 ccs of oxygen absorbers. Shows the initial fit of the logarithmic curve which although close, is not as good as it can be.

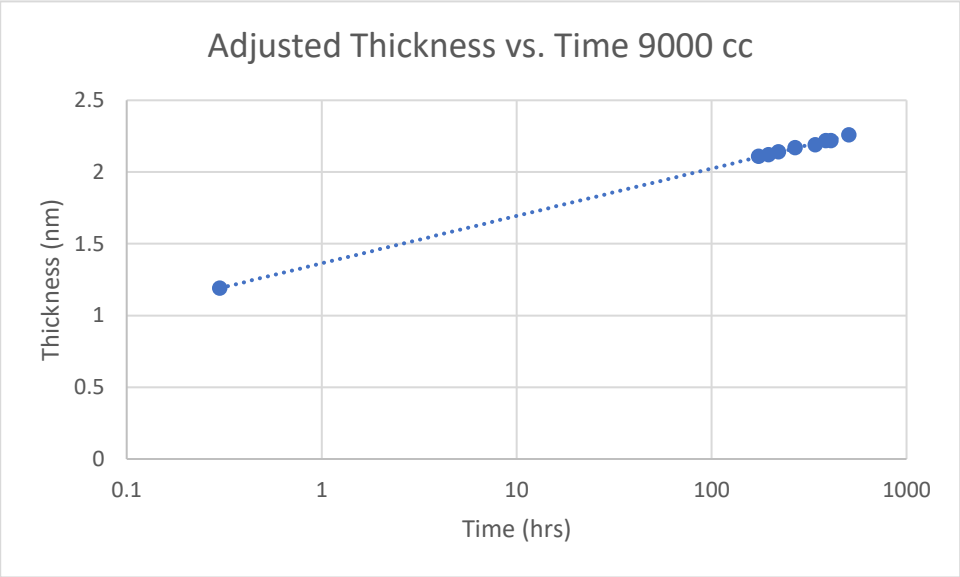

Figure 9: The thickness versus time plot for samples placed in 9000 ccs of oxygen absorbers shifted by a retardation value of 2.4±0.3.

In order to compare these calculated values, the RV of each sample as well as the average with error bars is plotted below (Fig. 10). The trends appear largely uniform within the expected error bounds, except for one 3000 cc sample and one 6000 cc sample. Both appear to have lower RV than the average.

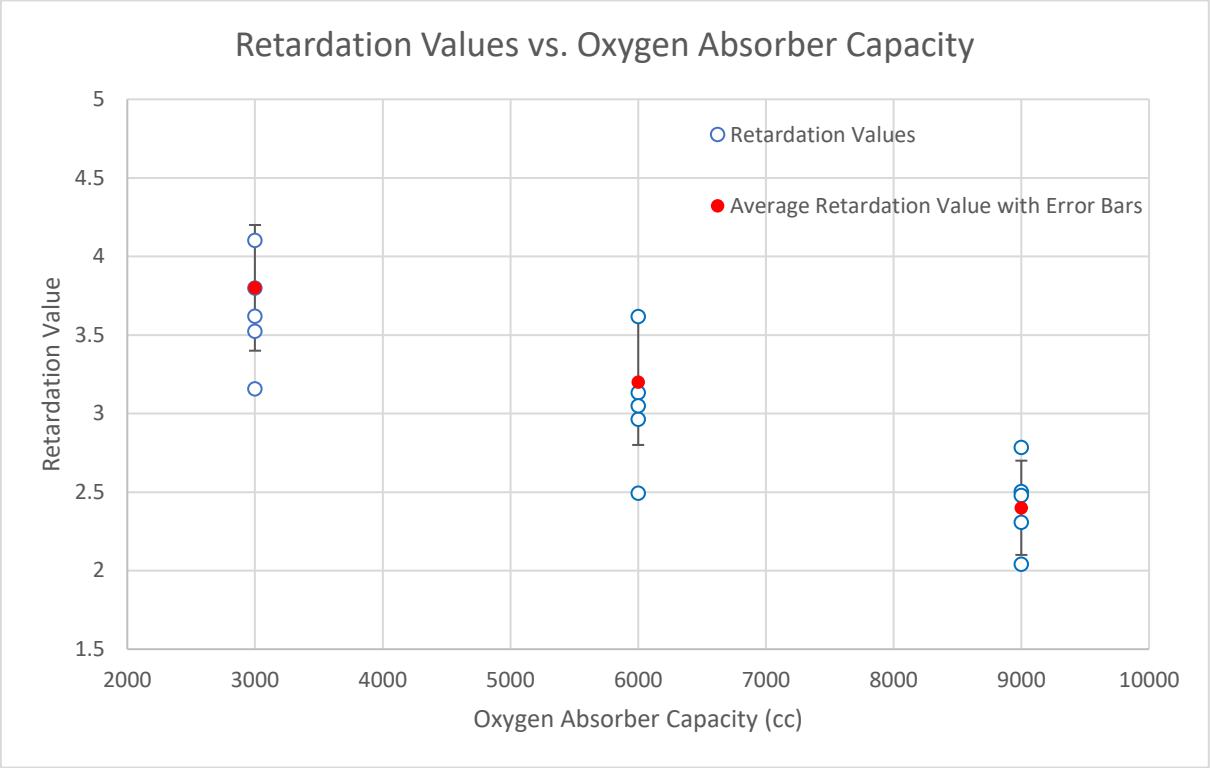

Figure 10: Each of the 15 sample's retardation values. The average RV for each oxygen absorber capacity is also shown along with the error bars to illustrate overlap in sample thickness as a function of ccs. Although none of the samples overlap significantly in RV, the 3000 cc and 6000 cc samples have outliers which follow trends similar to the other capacities.

3.3 Conclusions and Future Work

Curiously, the data appears to show that higher volumes of oxygen absorbers cause an increase in the oxidation rate of aluminum. Moreover, for seemingly having less than 100 ppm of oxygen inside the sealed bag, which is the environment oxygen absorbers create, there is still a substantial amount of oxide. The air is only comprised of 1/5 oxygen, meaning that a volume of 1600 ccs (the volume of the vacuum seal bags used to hold the samples) only theoretically needs

about 350 ccs of oxygen absorbers to reach a desired environment of <100 ppm oxygen concentration. The question then is why does more volume of oxygen absorbers appear to increase the oxygen concentration in the environment?

One possible explanation of this phenomenon is that aluminum has a higher bonding affinity than iron with oxygen. This leads oxygen to be more prone to reacting with aluminum rather than the iron. This could also mean that potentially, the iron is bonding with oxygen, then once inside the vacuum bag, the aluminum takes the oxygen bonded to iron. Preventative measures were taken to decrease the oxide reacted to iron before being subject to the environment by not opening the container with oxygen absorbers before the samples were finished so they all could be immediately put in the vacuum seal bag. However, the short amount of time could have been enough for the iron to oxidize slightly and coupled with the oxygen present inside the containers upon closing, it caused the aluminum to oxidize and the retardation values to be lower than expected.

These results still provide a retardation value up to 4, and coupled with thin film fluoride layers the potential to slow oxidation by four times the rate in air is valuable. This is especially true for cooperative experiments were slowing of oxidation between labs by that rate would lead to measurements being more uniform. The future work necessary to better understand results would be trying smaller oxygen absorber capacities closer to the minimum required value to effectively create a low oxygen environment to see if a lower capacity of oxygen absorbers continues to increase the retardation value.

Bibliography

Allred, D. D. (2017). Adding EUV reflectance to aluminum-coated mirrors for space-based observation. *SPIE*, 10395, 34.

Cichello, S. A. (2015). Oxygen absorbers in food preservation: a review. *Journal of food science and technology*.

Davis, A. A. (2017). *Oxidation of Aluminum Under Various Thicknesses of Aluminum Flouride.* B.S. Thesis. Brigham Young University.

Egan, A. E. (2017). The development and characterization of advanced broadband mirror coatings for the far-UV. *SPIE*.

Fleming, B. Q. (2017). Advanced environmentally resistant lithium flouride mirror coatings for the next generation of broadband space observatories. *Applied Optics*, 56(36), 9941-9950.

Grimblot, J. (1982). II. Oxidation of Al films. *J. Electrochem Soc.*, 129(10), 2369.

Hennessy, J. J. (2016). Ultraviolet optical properties of aluminum flouride thin films deposited by atomic layer deposition. . *Journal of Vacuum Science & Technology*, 34(1), 01A120.

Hunter, W. R. (1971). Reflectance of Aluminum Overcoated with MgF(2) and LiF in the Wavelength Regions from 1600 A to 300 A at Various Angles of Incidence. *Applied Optics*, 10(3), 540-544.

Larruquert, J. I. (1995). Far-ultraviolet reflectance measurements and optical constants of unoxidized aluminum films. *Applied optics*, 34(22), 4892-4899.

Madden, R. P. (1963). On the vacuum-ultraviolet reflectance of evaporated aluminum before and during oxidation. *Journal of the Optical Society of America*, 53(5), 620-625.

Méndez, J. A. (2000). Preservation of far-UV aluminum reflectance by means of overcoating with C 60 films. *Applied Optics*, 39(1), 149-156.

Miles, M. (2017). *Evaporated Aluminum Flouride as a barrier Layer to Retard Oxidation of Aluminum Mirrors.* Theses and Dissertations, Brigham Young University.

National Academies of Sciences, Engineering, and Medicine. (2021). *Pathways to Discovery in Astronomy and Astrophysics for the 2020s.*

Turley, R. S. (2017). Bare Aluminum Oxidation. *BYU Scholars Archive*.

Index